



King's Research Portal

DOI:

[10.1038/nchembio.2008](https://doi.org/10.1038/nchembio.2008)

Document Version

Peer reviewed version

[Link to publication record in King's Research Portal](#)

Citation for published version (APA):

Müller, M., Fierz, B., Bittova, L., Liszczak, G., & Muir, T. W. (2016). A two-state activation mechanism controls the histone methyltransferase Suv39h1. *Nature Chemical Biology*, 12(3), 188-193.

<https://doi.org/10.1038/nchembio.2008>

Citing this paper

Please note that where the full-text provided on King's Research Portal is the Author Accepted Manuscript or Post-Print version this may differ from the final Published version. If citing, it is advised that you check and use the publisher's definitive version for pagination, volume/issue, and date of publication details. And where the final published version is provided on the Research Portal, if citing you are again advised to check the publisher's website for any subsequent corrections.

General rights

Copyright and moral rights for the publications made accessible in the Research Portal are retained by the authors and/or other copyright owners and it is a condition of accessing publications that users recognize and abide by the legal requirements associated with these rights.

- Users may download and print one copy of any publication from the Research Portal for the purpose of private study or research.
- You may not further distribute the material or use it for any profit-making activity or commercial gain
- You may freely distribute the URL identifying the publication in the Research Portal

Take down policy

If you believe that this document breaches copyright please contact librarypure@kcl.ac.uk providing details, and we will remove access to the work immediately and investigate your claim.

Reconstitution of heterochromatin spreading on designer chromatin reveals a two-state activation mechanism for the histone methyltransferase Suv39h1

Authors

Manuel M. Müller¹, Beat Fierz¹†, Lenka Bittova¹, and Tom W. Muir^{1*}

Affiliations

¹Department of Chemistry, Princeton University, Princeton, NJ 08544, United States.

*Correspondence to: muir@princeton.edu.

†Current address: Ecole polytechnique fédérale de Lausanne, CH-1015 Lausanne, Switzerland.

ABSTRACT

Specialized chromatin domains contribute to nuclear organization and the regulation of gene expression. Gene-poor regions are demarcated by the activity of the histone methyltransferase, Suv39h1, which di- and trimethylates lysine 9 of histone H3 (H3K9me_{2/3}). A positive feedback loop is hardwired into the domain architecture of Suv39h1, enabling it to spread H3K9me_{2/3} over extended heterochromatic regions. However, little is known about how feedback loops operate on complex biopolymers such as chromatin, in part because of the difficulty in obtaining suitable substrates. Here we describe the synthesis of multi-domain 'designer chromatin' templates and their application to dissecting Suv39h1 regulation. We uncover a two-step activation switch where H3K9me₃ recognition and subsequent anchoring of the enzyme to chromatin allosterically promotes methylation activity, and confirm that this mechanism contributes to chromatin recognition in cells. We propose that this mechanism serves as a paradigm in chromatin biochemistry since it enables highly dynamic sampling of chromatin state combined with targeted modification of desired genomic regions.

MAIN TEXT

Hierarchical organization within the nucleus enables cell-type specific interpretation of eukaryotic genomes. A fundamental feature of this architecture is the packing of DNA through cationic protein scaffolds, histone octamers, to yield nucleosome core particles¹. Post-translational modifications (PTMs) of histones can affect both the structure and function of chromatin regions through biophysical and biochemical means². For instance, the formation of tightly compacted chromatin domains across gene-poor regions (heterochromatin) is catalyzed by the histone methyltransferase Suv39h1 (KMT1A) and the closely related enzyme Suv39h2 (KMT1B), which install the classic heterochromatin modifications, H3K9me2/3 (**Fig. 1a**)^{3,4}. These histone marks recruit heterochromatin protein 1 (HP1) to mediate downstream silencing of affected chromatin domains⁵⁻⁷. Importantly, for proper nuclear organization, heterochromatin must be propagated by Suv39h1 and HP1 over large, defined regions of the genome – a process referred to as spreading⁸. Excessive or insufficient spreading results in genome instability⁹ and can cause diseases due to gene mis-regulation¹⁰.

Suv39h1 contains a chromodomain (CD) capable of binding the product of its own reaction, H3K9me2/3 (**Fig. 1a**)¹¹. The CD is important for chromatin binding and methyltransferase activity of Suv39h1 in cells^{11,12}, suggesting that a positive feedback loop controls heterochromatin formation. Indeed, semi-synthetic dinucleosome substrates have been employed to demonstrate that Clr4, the yeast homolog of Suv39h1, is stimulated by H3K9me3 marks *in vitro*¹³. Despite these insights, the mechanism of how the CD and the enzymatic core cooperate to enact propagation of H3K9me3 along the chromatin fiber has

remained enigmatic, especially for the mammalian spreading system where the regulation of the methyltransferase has yet to be explored in a defined biochemical system. Allosteric regulation of enzymes is an important aspect of many processes in chromatin biochemistry^{14,15}, and particularly interesting from an enzymology standpoint given that, in this case, the substrate and allosteric modulator are tethered in a heteropolymeric template. This feature raises questions relating to the geometry of the feedback system, which have largely remained unexplored.

To address these issues, we engineered nucleosome arrays with distinct subdomains, resembling the complex architecture of chromatin in cells¹⁶. We have applied this type of ‘designer chromatin’¹⁷ to reconstitute Suv39h1-dependent H3K9me3 spreading *in vitro*, providing insight into the geometric and enzymatic mechanism of this process. We found that Suv39h1 preferentially takes small spreading steps within a single chromatin template, but long-range heterochromatin propagation can occur upon chromatin folding. Furthermore, our experiments unveiled that Suv39h1 is controlled by an unanticipated two-step activation switch involving a latent chromatin binding feature.

RESULTS

Synthesis of multi-domain designer chromatin

To enable biochemical reconstitution of Suv39h1-dependent heterochromatin spreading, we devised the synthesis of 12-mer nucleosome arrays that contain a stretch of four initiating nucleosomes, followed by a block of eight substrate nucleosomes (**1**, **Fig. 1b**). Notably, homogeneous arrays of this length have served for numerous biochemical and biophysical studies as they encompass the length of a small gene^{17,18}. Moreover,

tetranucleosomes appear to be a defined subunit of higher order chromatin structure observed in models derived from electron microscopy¹⁹ and crosslinking in cells²⁰. Inspired by methods for the synthesis of heterotypic di- and tetranucleosomes^{21,22}, we chose to use DNA ligation to assemble chemically defined arrays from homogeneous 4-mer building blocks (**Fig. 1b**). The 4-mers were prepared from histone octamers (consisting of unmodified, recombinant histones and semi-synthetic H3K9me3, **Supplementary Fig. 1**) and four repeats of a strong nucleosome positioning sequence²³, separated by 30 bp linker DNA (**Supplementary Fig. 2**). To enable directed ligation, each building block was furnished with specific, non-palindromic 3- or 4-bp overhangs. A one-pot ligation of all three fragments, followed by purification by MgCl₂-precipitation and sucrose gradient centrifugation provided 12-mer array **1** in good purity (**Fig. 1c** and **Supplementary Fig. 3**). Ligations were specific as the omission of fragments leads to the expected truncated products (**Fig. 1d**), and digestion of purified arrays revealed that the H3K9me3 marks were retained at their designated location (**Fig. 1e**).

An *in vitro* heterochromatin spreading system

With designer chromatin substrates in hand, we turned our attention to the issue of reconstituting H3K9me_{2/3} spreading *in vitro*. Recombinant human Suv39h1 was isolated from an insect cell expression system (**Supplementary Fig. 4**) and used in a scintillation-based histone methyltransferase (HMT) assay employing ³H-SAM and a designer chromatin substrate. Consistent with a functional positive feedback loop, the presence of the H3K9me₃ priming domain within array **1** led to robust stimulation of HMT activity in comparison to control substrate **2** which lacks this domain (**Fig. 2a** and **Supplementary**

Fig. 5) - this corresponds to a 25-fold activation when considering available methylation sites between substrates. Importantly, a nucleosome array carrying H3K9me3 throughout (3) was not further methylated under the same conditions, in line with the expected specificity of Suv39h1 (**Fig. 2a**).

To explore whether this spreading phenomenon can operate in an inter-array fashion, we performed an HMT assay using a 1:2 mixture of homogeneous arrays with (3) and without (2) the H3K9me3 mark. The absolute concentrations of priming vs. substrate sites match those of array 1. Under the conditions of the assay, arrays are predominantly self-assembled (**Supplementary Fig. 6**), thus resembling densely packed chromatin from cells²⁴. We observed elevated levels of Suv39h1 activity on this substrate mixture compared to the individual components (**Fig. 2a**), indicating that HMT activation can extend across chromatin fibers, consistent with physical models of heterochromatin spreading²⁵. As expected, *trans* spreading is strongly reduced when the assay is performed under conditions where chromatin assembly is unfavorable (0.5 mM MgCl₂, **Supplementary Figs. 6 and 7**). Even when chromatin is self-assembled (5 mM MgCl₂), inter-array activation cannot account for all the HMT activity seen with heterotypic array 1 (at most ~40%) implying that the *cis* spreading mechanism still dominates in this case.

We next turned our attention to the geometry of Suv39h1-catalyzed *cis*-spreading. This investigation was enabled by designer chromatin arrays 4 and 5 that contain three distinct subdomains; an H3K9me3 priming region, an unmodified substrate region and a region containing H3K9R nucleosomes that serves as a barrier for Suv39h1 (**Figs. 1b and c**). Higher levels of HMT activity were observed on array 4, which contains the substrate region proximal to the priming region, compared to array 5, which has the reverse

configuration (**Fig. 2a**). This result demonstrates that Suv39h1 prefers small spreading steps. To test whether residual activity on distal nucleosomes (as seen in array **5**) is due to *trans*-spreading or the possibility of Suv39h1 reaching over 4 intermittent nucleosomes, we analyzed the methylation distribution in a spreading reaction on array **1** in the presence of 0.5 mM MgCl₂. A unique *NcoI* restriction site in the array allowed us to interrogate the substrate regions proximal or distal to the priming site by digestion, followed by fluorography (**Fig. 2b** and **Supplementary Fig. 8**). Consistent with directional spreading, Suv39h1 activity is almost exclusively localized on nucleosomes proximal to the pre-installed H3K9me3 mark, with only a small amount observed on the distal subdomain. Collectively, these experiments establish the utility of our reconstituted system for probing PTM spreading and reveal that the presence of pre-installed H3K9me3 priming marks is sufficient to stimulate Suv39h1 activity on proximal nucleosomes.

The CD and N-terminus of Suv39h1, but not HP1, contribute to spreading activity *in vitro*

To gain further insight into the spreading mechanism, we compared the HMT activity of Suv39h1 variants on both designer chromatin array **1** as well as histone peptides (residues 1-20 of H3). As expected, a Suv39h1 variant with the active site mutation H324L was inactive on both substrates (**Fig. 2c**)³. Disabling the positive feedback loop through mutation of the chromodomain of Suv39h1 (W64A) has only a small effect on peptide substrates, in agreement with previous findings²⁶, but leads to a more profound reduction of activity on array **1** (**Fig. 2c**). We also investigated whether the N-terminus of the methyltransferase, known to interact with HP1²⁷, affects HMT activity. Interestingly, the Suv39h1 variant lacking the N-terminal 39 residues (Δ N) displays enhanced activity on

peptide substrates, but reduced activity on chromatin (**Fig. 2c**) suggesting that the N-terminus contributes to chromatin recognition and/or HMT activity.

Inclusion of recombinant HP1, which engages H3K9me3 through its own CD (**Supplementary Fig. 9**), in our spreading system did not lead to further stimulation of Suv39h1 activity on array **1** (**Fig. 2d**). By contrast, addition of HP1 actually reduced HMT activity for the Δ N variant of Suv39h1. This effect likely relates to competition between the two proteins for the available H3K9me3 binding sites¹³, which can presumably be alleviated by the direct interaction of HP1 with wild-type Suv39h1 but not the Δ N variant²⁷. Consistent with this idea, we observed no decrease in HMT activity when a mutant HP1 containing a defective CD (K44,W45A) was added to the assay system (**Fig. 2d** and **Supplementary Fig. 9**). Taken together, these data suggest that mammalian Suv39h1 is able to initiate the spreading of the H3K9me3 mark through a mechanism that is independent of HP1, but that requires both the CD and N-terminal region of the enzyme.

Allosteric activation of Suv39h1 on chromatin substrates

Conceivably, H3K9me3 could stimulate Suv39h1 activity through recruitment to chromatin, allosteric activation of the enzymatic activity, or a combination of both. These options were explored by performing the HMT assay on unmodified peptide or unmodified nucleosome array (**2**) substrates in the presence of an additional H3K9me3-containing peptide. We observed no *trans*-stimulation of HMT activity in the context of the H3 peptide substrate (**Fig. 3a**). In sharp contrast, addition of H3K9me3 peptide strongly enhanced HMT activity on unmodified chromatin (**Fig. 3a**). This stimulation required an intact chromodomain within Suv39h1, which presumably functions as a sensor for the

methylation mark (**Fig. 3b**). More surprisingly, the H3K9me3 peptide was also unable to stimulate the ΔN variant of Suv39h1, further implicating this region of the enzyme in the spreading feedback mechanism.

The ability of H3K9me3 peptides to trans-activate Suv39h1 activity on chromatin reveals an allosteric component to the spreading process. Because this effect does not extend to peptide substrates, we asked whether the H3K9me3 mark induces chromatin binding by the methyltransferase. To this end, we developed a chromatin binding assay wherein nucleosome arrays containing either H3K9me0 or H3K9me3 were incubated with wild-type Suv39h1 or its variants in the presence of 5 mM MgCl₂, causing self-assembly and precipitation of chromatin (**Supplementary Fig. 6**). Resuspension of the pellet in the absence of MgCl₂, followed by centrifugation to remove insoluble precipitates allowed us to assess the extent to which Suv39h1 associates with chromatin. Suv39h1 did not associate appreciably with unmodified chromatin array **2**, but readily bound to homogeneously H3K9-methylated arrays **3** (**Figs. 3c & d**). Importantly, chromatin association was strongly enhanced by H3K9me3 not only in *cis*, but also when this mark was added as a peptide in *trans*. Control experiments confirmed that chromatin binding depends on the H3K9me3 mark, and that in the absence of MgCl₂, chromatin and consequently also Suv39h1 remain in the supernatant. As expected, chromatin binding was attenuated when either the CD of Suv39h1 was crippled or the N-terminus removed, confirming their role in the spreading mechanism (**Fig. 3d**). Partial binding of the W64A variant to array **3** likely originates from residual affinity of the crippled CD to H3K9me3 (ref¹¹).

A Zn-finger like motif contributes to chromatin binding *in vitro* and *in vivo*

We noticed that the sequence of the Suv39h1 N-terminus displays a remarkable similarity to the N-terminal helix of the Zn-finger from the DNA-binding protein Gal4 (**Fig. 4a**). Consequently, we wondered whether Suv39h1 is capable of directly binding DNA and employed a pull-down assay with biotinylated 601 DNA to explore this idea. Only weak interactions between Suv39h1 and DNA were observed in the presence of the H3K9me0-peptide (**Supplementary Fig. 10**), which is consistent with a previous biochemical study²⁸. However, DNA binding was enhanced by the presence of the H3K9me3-peptide (**Supplementary Fig. 10**). Based on this, we next investigated whether this N-terminal motif in Suv39h1 was important for function. Specifically, we prepared a variant where the postulated DNA binding residues (R24 and K27, **Fig. 4a**) are mutated to Ala. Chromatin binding of the R24,K27A double mutant was strongly diminished in the context of fully methylated array **3**, as well as unmodified array **2** in the presence of stimulatory H3K9me3 peptide (**Fig. 4b**). Moreover, this double mutant exhibited severely compromised activity in HMT assays with array **1** and with array **2** in the presence of H3K9me3 peptide (**Fig. 4c**).

Finally, we tested whether the N-terminus of Suv39h1 contributes to chromatin binding in cells. To this end, Suv39h1-GFP fusions were transfected into NIH-3T3 cells, and the subnuclear localization of the constructs visualized by fluorescence microscopy. Wild-type Suv39h1-GFP and the R24,K27A mutant localize to dense heterochromatin foci, whereas a variant lacking the entire N-terminus (Δ N) is diffusely distributed through the nucleus (**Fig. 5a**). The difference in localization between the R24,K27A and the Δ N variant presumably reflects the ability of the former, but not the latter, to interact with HP1 (**Supplementary Fig. 11**)^{12,27,29}.

Fluorescence recovery after photobleaching (FRAP) confirmed that wild-type Suv39h1 exchanges at the timescale of seconds, with a subpopulation remaining immobile on the timescale of minutes, in agreement with previous reports^{30,31}. As expected, exchange occurs more readily in euchromatin than in heterochromatin (**Fig. 5b**). The ΔN variant interacts with chromatin only transiently, as reflected by the short residence time and the complete recovery (**Fig. 5b**), consistent with its inability to interact with HP1 (**Supplementary Fig. 11**)²⁷ as well as the reduced chromatin binding we observed *in vitro*. Notably, deletion of the N-terminus of Suv39h1 has also been shown to derepress major satellite repeats *in vivo* under steady-state conditions²⁹. Critically, the R24,K27A mutant of Suv39h1 exhibits more extensive exchange than the wild-type enzyme in both euchromatin and heterochromatin, presumably reflecting a loss in chromatin binding despite the presence of an intact chromodomain and the retention of HP1 binding ability (**Fig. 5b, Supplementary Fig. 11**). These results support the idea that specific residues present in the putative Zn-finger-like motif contribute to chromatin binding *in vivo*.

DISCUSSION

Although the heteropolymeric nature of chromatin has long been recognized¹⁶, few model systems have been established to test in a controlled manner how information (for example a histone PTM) is interpreted as a function of the location relative to a reporter site. One approach to this problem has been to artificially tether chromatin-modifying enzymes to specific genomic loci and then analyze the chromatin state and transcriptional output in the vicinity of the targeted enzymes^{32,33}. However, cell-based approaches of this type, while informative, do not establish direct causal relationships. Hence, there is a

pressing need for compositionally defined *in vitro* facsimiles of cellular chromatin that can be used to fully understand molecular mechanisms attendant to processes such as spreading^{34,35}. In this study, we have developed a means to access semi-synthetic designer chromatin that mimics natural chromatin with unprecedented detail in terms of array length and composition. The tripartite nature of arrays **1**, **4** and **5** enables incorporation of up to three distinct chromatin states at the level of tetranucleosomes, important subunits of chromatin structure^{19,20}. As such, these arrays promise to aid in elucidating the spatial determinants of how (far) histone modifications control chromatin structure and function, exemplified here by their application to investigate the enzymology of heterochromatin spreading.

Collectively, our biochemical data converge on a two-stage activation mechanism for Suv39h1 (**Fig. 5c**). In our model, Suv39h1, inactive in its free form, first samples chromatin through its chromodomain. Recognition of H3K9me3 then allosterically activates a latent DNA- and/or chromatin binding motif to anchor the enzyme to chromatin, likely involving a Zn-finger-like segment at the N-terminus. This second step in turn stimulates H3K9 methylation, specifically targeted to spatially close nucleosomes due to the multivalent nature of Suv39h1's chromatin engagement. This model features a highly mobile state of Suv39h1, characterized by low HMT activity to quickly sample chromatin states that can convert into an immobile population, engaging chromatin with its chromodomain and N-terminus. It complements orthogonal pathways to recruit and activate Suv39h1 for initiation of heterochromatin spreading, such as binding to RNA transcripts²⁸ or heterochromatin proteins^{27,33,36}.

Previously, Narlikar and co-workers have proposed a 'guided state' mechanism for spreading by Clr4, the yeast homolog of Suv39h1¹³. In this model, Clr4 binds to the chromatin template independent of the presence of H3K9me3, but is able to use the mark to reposition its active site, thus increasing the methyltransferase activity. Our studies of the reconstituted mammalian spreading system reveal that the H3K9me3 mark can allosterically activate Suv39h1 on chromatin. Here, the N-terminus of Suv39h1 acts as an anchor, thus strengthening the interaction with the substrate. The difference in mechanism most likely arises because of differences in the domain architecture in the respective enzymes (**Supplementary Fig. 12**). Clr4 does not contain any N-terminal extension, thus lacking the anchor present in Suv39h1. The connection between the CD and the SET domain also varies dramatically between the two homologs: the mammalian enzyme contains a 13-residue linker between the extended C-terminal helix of the CD and the N-terminal helix of the pre-SET domain^{37,38}, whereas the yeast enzyme features a >100 amino acid insertion at that position³⁹.

How are chromatin binding and activation of catalysis coupled in Suv39h1? The significantly increased activity of the Δ N variant on peptide substrates (**Fig. 2c**) hints at the intriguing possibility that the N-terminus auto-inhibits the SET domain, either allosterically or through direct binding. Upon chromatin binding, auto-inhibition is relieved, thus increasing the HMT activity. This effect could explain the difference in activity between the wild-type enzyme, the Δ N variant and the R24,K27A mutant on chromatin substrates (**Supplementary Fig. 13**). The latter exhibits low HMT activity because it is auto-inhibited and cannot engage chromatin. By contrast, the Δ N variant suffers from poor chromatin

binding, but displays intermediate catalytic proficiency because it is not auto-inhibited. Structural studies on the full-length enzyme might shed light on this issue.

We propose that the 2-state mechanism delineated above represents a common theme in chromatin biochemistry. Firstly, coupling of fast sampling of the chromatin environment with strong *local* activation of enzymatic activities at designated regions through a positive feedback loop provides an ideal mechanistic foundation for the formation of dynamic PTM domains. Moreover, many histone-modifying enzymes contain subunits that bind their respective products. Prominent examples include the methyltransferases PRC2 (which is also regulated through interactions with nucleic acids), G9a, and GLP^{14,40}, the acetyltransferases p300 and GCN5^{41,42}, and the demethylase KDM5A¹⁵. Sophisticated designer chromatin substrates of the type generated herein provide a foundation on which to test these ideas further.

ONLINE METHODS

Synthesis of hH3.1K9me3

Homogeneously modified hH3.1K9me3 (H3K9me3) was prepared by protein semi-synthesis according to previously published procedures⁴². Briefly, the N-terminal tail encompassing residues 1-28 and the K9me3 mark was synthesized on solid phase with a C-terminal diaminobenzoic acid moiety. This handle enabled facile conversion of the cleaved peptide into an α -thioester for native chemical ligation⁴³. Trimethyllysine at position 9 was incorporated using Fmoc-Lys(me₃,Cl)-OH. The C-terminal residue, Fmoc-Ser(tBu)-OH, was coupled to diaminobenzoic acid in solution as described⁴³, and subsequently loaded onto a rink amide ChemMatrix resin. SPPS was carried out using standard Fmoc-protocols (see above). Upon completion of the peptide synthesis, the diaminobenzoyl linker was activated by acylation with p-nitrophenylchloroformate for 2 x 40 min. at room temperature, followed by incubation with 0.5 M DIPEA in DMF to yield a cyclic N-acylurea intermediate. The peptides were then cleaved from the resin and deprotected with TFA/triisopropylsilane (TIS)/H₂O (95:2.5:2.5) for 3 h, precipitated with cold ether and collected by centrifugation. Crude peptides were then converted into α -thioesters by incubation in 100 mM phosphate buffer, pH 7.5 containing 150 mM 2-mercaptoethanesulfonate (MESNa) for 1 h at room temperature and purified by RP-HPLC on a preparative scale using a 5-20% B gradient over 60 min. The resulting peptide was characterized by ESI-MS: (M+H)⁺ observed: 3,165 Da; expected: 3,165 Da.

The C-terminal fragment of H3.1 (encompassing residues 29-135 and containing the mutations A29C, C96A, and C110A) was produced in *E. coli* as a SUMO fusion as previously

described⁴². The protein was isolated from inclusion bodies and purified by Ni-NTA chromatography under denaturing conditions. Upon refolding of SUMO, the fusion protein was incubated with Ulp1 SUMO protease, and the cleaved histone fragment purified by RP-HPLC (45-60 % HPLC buffer B gradient, 20 mL/min, over 60 min). The final product was characterized by ESI-MS: H3.1 (29-135, A29C,C96A,C110A) (M+H)⁺ observed: 12,263 Da, calculated: 12,261 Da).

The α -thioester (4.5 mg, 1.4 μ moles) was ligated to the C-terminal fragment (8 mg, 0.65 μ moles) in 650 μ L ligation buffer (100 mM sodium phosphate pH 7.5 containing 6 M guanidinium chloride (GdmCl), 30 mM 4-mercaptophenylacetic acid (MPAA) and 60 mM TCEP) for 6 hours at RT. The product was purified by reverse phase HPLC and subjected to radical desulfurization⁴⁴ with 40 mM glutathione, 200 mM TCEP, 16 mM VA-61 at 37 °C overnight. hH3.1K9me3 was purified by reverse phase HPLC in 20 % isolated yield (2 mg) over 2 steps: (M + H)⁺ observed: 15,250 Da; expected 15,251 Da (**Supplementary Fig. 1**).

Octamer formation

Octamers containing the desired histone variants (wild-type H3, H3K9me3, H3K9R) were prepared as previously described⁴⁵. Briefly, recombinant and semi-synthetic histones were dissolved in histone unfolding buffer (20 mM Tris-HCl, 6 M GdmCl, 0.5 mM DTT, pH 7.5), combined (1.1 eq H2A, 1.1 eq H2B, 1.0 eq H3 variant, 1 eq H4), and the total histone concentration was adjusted to 1 mg/mL. Octamers were assembled by dialysis at 4 °C against 3x 1 L of octamer refolding buffer (10 mM Tris-HCl, 2 M NaCl, 0.5 mM EDTA, 1 mM DTT, pH 7.5) and subsequently purified by size exclusion chromatography on a Superdex

S200 10/300 column. Fractions containing octamers were combined, concentrated, diluted with glycerol to a final 50 % v/v and stored at -20 °C.

Preparation of nucleosomal DNA

Dodecameric repeats of the 601 sequence²³ separated by 30 bp linkers were produced from pWM530 by *EcoRV* digestion and PEG-6000 precipitation according to previously published procedures⁴⁶. Tetrameric repeats (A4-1, A4-2, A4-3) were generated from a plasmid harboring the 601 sequence using a standard PCR- and restriction enzyme-based molecular cloning approaches. Full sequences of the tetrameric repeats, including the location of the *DraIII*, *BsaI* and *AlwNI* non-palindromic sites used in chromatin assembly, are provided in **Supplementary Fig. 2**. Note, for the central segment, A4-2, peripheral *NdeI* and *NcoI* restriction sites were included to enable selective cleavage of the resulting arrays for analytical purposes. The 4-mer repeats were excised from the respective WM530-based vectors with *AlwNI* and *BsaI* (A4-1) or *BsaI* and *DraIII* (A4-2, A4-3). Subsequently, the backbone was digested with *EcoRV* to enable selective PEG precipitation of the 4-mer repeats. Typically, two or three iterations of precipitation were conducted. The purified DNA was dissolved in TE buffer and stored at -80 °C in aliquots.

Biotinylated 601 DNA was prepared by PCR using Biotin-CTGGAGAATCCCGGTGCCGA and ACAGGATGTATATATCTGACACG as primers and a 601 DNA template on a 4.8 mL scale. Products were purified with a Qiagen PCR purification kit and ethanol precipitation. 5-Methylcytosine was incorporated by including 0.2 mM 5-me-dCTP instead of dCTP in the PCR mix.

Formation of homotypic nucleosome arrays

Homotypic dodecameric arrays were assembled from purified octamers (containing either recombinant H3 (Array 2) or semi-synthetic H3K9me3 (Array 3)) and recombinant DNA in the presence of buffer DNA by salt gradient dialysis as previously described⁴⁷. Homotypic tetramers were prepared in the absence of buffer DNA on a 50-200 pmole scale. The resulting arrays were purified by sucrose gradient centrifugation (5-40% sucrose in 4.5 mL TEK buffer (10 mM Tris, pH 8, 0.1 mM EDTA, 10 mM KCl)) for 5h at 40,000 rpm in a 55Ti Rotor (Beckman Coulter) at 4 °C. Fractions containing saturated tetrameric arrays were pooled, concentrated on a Vivaspin 500 centrifugal concentrator (30 kDa cutoff) and washed three times with TEK containing 0.2 mM PMSF to remove the sucrose. Six different types of homotypic tetramers were produced: A4-1 wt H3; A4-2 wt; A4-3 wt; A4-1 H3K9R; A4-2 H3K9R; A4-3 H3K9me3. Recoveries for purified fragments ranged from 20-60 %.

Formation of heterotypic nucleosome arrays by DNA ligation

Heterotypic arrays were synthesized by DNA ligation from homotypic fragments. Unique non-palindromic overhangs generated by *AlwNI*, *BsaI* and *DraIII* enabled one-pot, site-specific ligation. Typically, 1.25 equivalents of outer fragments (40 nM per 601 site) and 1.0 equivalent of the middle segment (32 nM per 601 site) were joined using T4 DNA ligase (NEB, 5 U/μL) in 70 mM Tris-HCl, pH 7.5 containing 6 mM MgCl₂, 1 mM ATP and 10 mM DTT. After 2h at 16 °C, the reactions were centrifuged (17,000 g for 10 min at 4 °C). The pellet containing predominantly 12-mer products was redissolved in TEK buffer and subjected to sucrose gradient purification as described for the 4-mer intermediates. Isolated yields were typically around 20 %.

Array integrity was assessed by *ScaI*- and MNase digestion. The former was performed with 0.9 pmoles 601 site and 500 U *ScaI* in 3.5 μ L 10 mM Tris-HCl, pH 7.5 containing 0.1 M KCl, 0.5 mM MgCl₂, 1 mM DTT for 4h at RT. Digested products were analyzed by native gel electrophoresis on a 5% acrylamide gel. MNase digestion was performed with 0.9 pmoles 601 site and 0.2 U MNase in 20 μ L 10 mM Tris-HCl, pH 7.5 containing 1 mM CaCl₂ at 4 °C. The reaction was quenched with SDS after 30 s, and the digested DNA was isolated with a Qiagen PCR purification kit and analyzed by acrylamide gel electrophoresis. Representative examples of *ScaI* and MNase digestions of dodecameric arrays **1-3** are shown in **Supplementary Figure 3**.

The integrity of H3K9me3 domains installed through chromatin ligations were tested by restriction digestion, native gel electrophoresis and western blotting. Specifically, 0.125 pmoles array **1** (1 pmoles H3K9me3 and 2 pmoles of unmodified H3 on the histone level) were incubated for 1 hour at room temperature in 1x digestion buffer (10 mM Tris, pH 8, 50 mM KCl, 1 mM MgCl₂) in the presence of 10 U *NdeI* or *NcoI*. Subsequently, array fragments were separated by native gel electrophoresis (2 % acrylamide, 1% agarose), and transferred to a PVDF membrane on a semi-dry blotter in the absence of SDS and MeOH. The resulting blots were developed with anti-H3K9me3 antibodies (Abcam, ab8898).

Cloning, expression, and purification of Suv39h1

The gene coding for Suv39h1 was obtained from Open Biosystems (MHS1011-61443) and subcloned into a pFastBac vector (Life Technologies) with an N-terminal Flag Tag. Variants were produced by site directed mutagenesis using the QuikChange Site-Directed Mutagenesis kit (Agilent). Bacmids were generated in DH10Bac cells according to

manufacturer's instructions and transfected into Sf-9 cells. Proteins were produced in Sf-9 cells infected with desired baculovirus constructs in Sf-900 III serum-free media on a 50-500 mL scale in shaker flasks. After 2 days of infection, cells were harvested by centrifugation. The cells were either stored at -80 °C or directly lysed by dounce homogenization in lysis buffer (20 mM Tris-HCl, 500 mM NaCl, 4 mM MgCl₂, 0.4 mM EDTA, 20% glycerol, 1 mM PMSF, 2 mM DTT, pH 7.9) and the solution cleared by centrifugation. The soluble extracts were incubated with anti-Flag M2 affinity gel (100 µL resin per 100 mL cell culture) in wash buffer (20 mM Tris, pH 7.9, 150 mM NaCl, 2 mM MgCl₂, 0.2 mM EDTA, 15% (v/v) glycerol, 0.1% NP-40, 1 mM PMSF, 1 mM DTT) for 1 hour at 4 °C. The resin was collected by centrifugation and washed three times with wash buffer. Bound proteins were subsequently eluted in wash buffer containing 0.25 mg/mL Flag peptide (2x 20 min at 4 °C). Eluted fractions were concentrated using Vivaspin 500 filters (10 kDa MW cutoff), and stored at -80 °C. Wild-type and mutant Suv39h1 were analyzed by SDS-PAGE and silver staining (**Supplementary Fig. 4a**) and/or western blotting (**Supplementary Fig. 4b**).

Histone methyltransferase assays

The methyltransferase activity of Suv39h1 and its variants was measured using a scintillation based assay. Typically, arrays (40 nM 601 site) were incubated with approximately 10 nM Suv39h1 in 10 µL HMT buffer (50 mM Tris-HCl, pH 8.5 containing 5 mM MgCl₂, 5 mM DTT, 1 mM PMSF) in the presence of 1.4 µM ³H-S-Adenosylmethionine (³H-SAM Perkin Elmer, Waltham, MA) for 2 h at room temperature. Note that under these conditions, arrays are reversibly self-assembled. Reactions were quenched by spotting on

Whatman P81 phosphocellulose filter discs (Sigma). The filters were dried for 1 h at RT, washed 3x with 0.2 M NaHCO₃, pH 9, and finally dried on a gel dryer for 30 min at 40 °C. Scintillation counting was performed with 1 mL Ultima Gold scintillation cocktail on a MicroBeta² scintillation counter (Perkin Elmer). Alternatively, 10 μM H3(1-20) peptide was used as substrates instead of nucleosome arrays. Where indicated, HP1 or its variants were added at 1 μM. When appropriate, H3(1-20)K9me3 peptide was added at 0.2 μM, unless otherwise stated.

To determine the location of HMT activity on array **1**, an HMT reaction was performed as above, but with higher concentrations of arrays (75 nM 601 site), Suv39h1 (15 nM) and 2.1 μM ³H-SAM in 5 μL HMT buffer containing 0.5 mM MgCl₂. The lower concentration of Mg²⁺ facilitates downstream analysis, and reduces chromatin self-assembly, ensuring that spreading occurs in an intra-array fashion. After intervals of 15, 30, 60 and 130 min at RT, 10 μL of digestion buffer containing 20 U of *NcoI* and 200 μM cold SAM were added. Digestions were allowed to proceed for 15 min at RT. Subsequently, the resulting array fragments (an 8-mer containing the pre-installed H3K9me3 marks and the adjacent 4 nucleosomes and a 4-mer containing the four nucleosomes distal to the pre-modified sites) were resolved by native gel electrophoresis (1% agarose and 2 % acrylamide). Gels were stained with Sybr Gold (Invitrogen), followed by fixing (40 % EtOH, 10 % AcOH, 45 min, RT) and incubation in Amplify solution (GE healthcare, 30 min, RT). Next, the gels were dried (2 h, 70 °C) and ³H-methyl incorporation was visualized by fluorography using XAR films. Bands corresponding to the 8-mer and 4-mer fragments were quantified by densitometry and relative values of ³H-incorporation were normalized by the total Sybr Gold signal in each lane. Time courses were conducted in duplicate.

Chromatin self-assembly assay

Self-assembly of chromatin in HMT assay buffer was assessed by incubating dodecameric arrays (40 nM 601 site) in 10 μ L HMT buffer with varying concentrations of $MgCl_2$ (0-5 mM) for 10 min at 4 $^{\circ}C$. Array aggregates were pelleted by centrifugation (10 min at 17,000 g at 4 $^{\circ}C$) and the amount of chromatin in the supernatant was determined by UV spectroscopy or Sybr Gold fluorescence (SpectraMax M3 plate reader, Molecular Devices, Sunnyvale, CA, at 495 nm excitation, 540 nm emission).

Chromatin-Suv39h1 binding assays

Binding of Suv39h1 variants to chromatin was evaluated with a co-precipitation assay. Dodecameric arrays (37.5 nM 601 site) were precipitated in the presence of approximately 10 nM Suv39h1 variant in 10 μ L HMT buffer (5 mM $MgCl_2$ unless stated otherwise) supplemented with 0.1 mg/mL BSA. Where appropriate, histone peptides were added at 0.2 μ M. After 30 min at RT, the samples were centrifuged for 10 min at 4 $^{\circ}C$. The supernatants were collected and the pellets were redissolved in 10 μ L TEK for 10 min at RT and centrifuged again for 10 min at 4 $^{\circ}C$ to remove insoluble species. Individual fractions were denatured with SDS-loading buffer (5 min at 95 $^{\circ}C$) and the presence of Suv39h1 variants analyzed by western blot (α -Flag).

DNA-binding assays

DNA binding of wild-type Suv39h1 was assessed by pulldown with biotinylated 601 DNA. 100 nM DNA was incubated with approximately 20 nM Suv39h1 in 10 μ L HMT buffer containing 0.2 μ M of the indicated peptide. After 30 min at RT, 20 μ L Dynabeads MyOne Streptavidin (Life Technologies) were added. Binding was allowed to proceed for 15 min.

Isolated beads were washed twice with 10 μ L HMT buffer, and subsequently treated with 10 μ L SDS loading buffer for 10 min at 95 °C. Bound Suv39h1 was detected by western blotting using an α -Flag antibody. Inputs correspond to 10 % of crude reaction mixtures.

Because crosstalk between DNA and histone methylation has been observed *in vivo*⁴⁸, we tested if DNA binding was sensitive to cytosine methylation by performing pull-downs using biotinylated 601 DNA that was prepared by PCR in the presence of 5-me-CTP. However, no change in pulldown was observed with DNA bait containing 5-methyl-Cytosine as compared to Cytosine.

Fluorescence microscopy and FRAP

NIH-3T3 cells were cultured as monolayers in Dulbecco's Minimal Essential Medium (Gibco BRL, Invitrogen Corporation, Carlsbad, CA, USA), supplemented with 10% fetal calf serum, antibiotics (penicillin, streptomycin), and L-glutamine at 37°C in an atmosphere of 5% CO₂ in air. Cells were transiently transfected with Suv39h1-GFP fusion constructs (in pcDNA-3.1) using lipofectamine 2000 (Life Technologies). After 6 hours of transfection, cells were trypsinized and applied to a MaTek glass bottom dish. Cells were allowed to attach and grow for another 24 hours before staining with Hoechst 33342 (5 μ g/ μ L). Fluorescence microscopy was performed on a Nikon R1 confocal microscope using a 100x/1.40 objective. Samples were kept at 37 °C in the presence of 5 % CO₂. DNA was visualized at 405 nm, GFP fusions at 488 nm. 5 frames were imaged before photobleaching was conducted on a 1 μ m circular spot with a 488 nm laser operating at 20 % (heterochromatin) or 100% intensity (euchromatin) for 120 ms. Recovery was monitored for 96 s at 2 s intervals. For visualization purposes, the resulting FRAP traces were fit to the

coupled binding-diffusion model of Sprague *et al.* using MATLAB (Mathworks, Natick, MA)⁴⁹.

REFERENCES

- 1 Kornberg, R. D. Structure of chromatin. *Annu Rev Biochem* **46**, 931 (1977).
- 2 Woodcock, C. L. & Ghosh, R. P. Chromatin higher-order structure and dynamics. *Cold Spring Harb Perspect Biol* **2**, 1 (2010).
- 3 Rea, S. *et al.* Regulation of chromatin structure by site-specific histone H3 methyltransferases. *Nature* **406**, 593 (2000).
- 4 Nakayama, J., Rice, J. C., Strahl, B. D., Allis, C. D. & Grewal, S. I. Role of histone H3 lysine 9 methylation in epigenetic control of heterochromatin assembly. *Science* **292**, 110 (2001).
- 5 Grewal, S. I. & Moazed, D. Heterochromatin and epigenetic control of gene expression. *Science* **301**, 798 (2003).
- 6 Lachner, M., O'Carroll, D., Rea, S., Mechtler, K. & Jenuwein, T. Methylation of histone H3 lysine 9 creates a binding site for HP1 proteins. *Nature* **410**, 116 (2001).
- 7 Noma, K.-i., Allis, D. C. & Grewal, S. I. S. Transitions in distinct histone H3 methylation patterns at the heterochromatin domain boundaries. *Science* **293**, 1150 (2001).
- 8 Talbert, P. & Henikoff, S. Spreading of silent chromatin: inaction at a distance. *Nature Rev Genet* **7**, 793 (2006).
- 9 Peters, A. *et al.* Loss of the Suv39h histone methyltransferases impairs mammalian heterochromatin and genome stability. *Cell* **107**, 323 (2001).
- 10 Hahn, M., Dambacher, S. & Schotta, G. Heterochromatin dysregulation in human diseases. *J Appl Physiol* **109**, 232 (2010).
- 11 Zhang, K., Mosch, K., Fischle, W. & Grewal, S. I. Roles of the Clr4 methyltransferase complex in nucleation, spreading and maintenance of heterochromatin. *Nat Struct Mol Biol* **15**, 381 (2008).

- 12 Melcher, M., Schmid, M., Aagaard, L., Selenko, P., Laible, G. & Jenuwein, T. Structure-Function Analysis of SUV39H1 Reveals a Dominant Role in Heterochromatin Organization, Chromosome Segregation, and Mitotic Progression. *Mol Cell Biol* **20**, 3728 (2000).
- 13 Al-Sady, B., Madhani, H. D. & Narlikar, G. J. Division of labor between the chromodomains of HP1 and Suv39 methylase enables coordination of heterochromatin spread. *Mol Cell* **51**, 80 (2013).
- 14 Margueron, R. *et al.* Role of the polycomb protein EED in the propagation of repressive histone marks. *Nature* **461**, 762 (2009).
- 15 Torres, I. O., Kuchenbecker, K. M., Nnadi, C. I., Fletterick, R. J., Kelly, M. J. & Fujimori, D. G. Histone demethylase KDM5A is regulated by its reader domain through a positive-feedback mechanism. *Nat Commun* **6**, 6204 (2015).
- 16 Rando, O. J. Global patterns of histone modifications. *Curr Opin Genet Dev* **17**, 94 (2007).
- 17 Müller, M. M. & Muir, T. W. Histones: at the crossroads of peptide and protein chemistry. *Chem Rev* **115**, 2296 (2015).
- 18 McGinty, R. K. & Tan, S. Nucleosome structure and function. *Chem Rev* **115**, 2255 (2015).
- 19 Song, F., Chen, P., Sun, D., Wang, M., Dong, L., Liang, D., Xu, R.-M., Zhu, P. & Li, G. Cryo-EM study of the chromatin fiber reveals a double helix twisted by tetranucleosomal units. *Science* **344**, 376 (2014).
- 20 Hsieh, T. H., Weiner, A., Lajoie, B., Dekker, J., Friedman, N. & Rando, O. J. Mapping nucleosome resolution chromosome folding in Yeast by Micro-C. *Cell* **162**, 108 (2015).
- 21 Zheng, C. & Hayes, J. J. Intra- and inter-nucleosomal protein-DNA interactions of the core histone tail domains in a model system. *J Biol Chem* **278**, 24217 (2003).
- 22 Blacketer, M. J., Feely, S. J. & Shogren-Knaak, M. A. Nucleosome interactions and stability in an ordered nucleosome array model system. *J Biol Chem* **285**, 34597 (2010).

- 23 Lowary, P. T. & Widom, J. New DNA sequence rules for high affinity binding to histone octamer and sequence-directed nucleosome positioning. *J Mol Biol* **276**, 19 (1998).
- 24 Hansen, J. C. Conformational dynamics of the chromatin fiber in solution: determinants, mechanisms, and functions. *Annu Rev Biophys Biomol Struct* **31**, 361 (2002).
- 25 Erdel, F., Müller-Ott, K. & Rippe, K. Establishing epigenetic domains via chromatin-bound histone modifiers. *Ann N Y Acad Sci* **1305**, 29 (2013).
- 26 Chin, H., Patnaik, D., Estève, P.-O., Jacobsen, S. & Pradhan, S. Catalytic properties and kinetic mechanism of human recombinant Lys-9 histone H3 methyltransferase SUV39H1: participation of the chromodomain in enzymatic catalysis. *Biochemistry* **45**, 3272 (2006).
- 27 Yamamoto, K. & Sonoda, M. Self-interaction of heterochromatin protein 1 is required for direct binding to histone methyltransferase, SUV39H1. *Biochem Biophys Res Commun* **301**, 287 (2003).
- 28 Porro, A., Feuerhahn, S., Delafontaine, J., Riethman, H., Rougemont, J. & Lingner, J. Functional characterization of the TERRA transcriptome at damaged telomeres. *Nat Commun* **5**, 5379 (2013).
- 29 Muramatsu, D., Singh, P., Kimura, H., Tachibana, M. & Shinkai, Y. Pericentric Heterochromatin Generated by HP1 Protein Interaction-defective Histone Methyltransferase Suv39h1. *J Biol Chem* **288**, 25285 (2013).
- 30 Müller-Ott, K. *et al.* Specificity, propagation, and memory of pericentric heterochromatin. *Mol Sys Biol* **10**, 746 (2013).
- 31 Krouwels, I. M., Wiesmeijer, K., Abraham, T. E., Molenaar, C., Verwoerd, N. P., Tanke, H. J. & Dirks, R. W. A glue for heterochromatin maintenance: stable SUV39H1 binding to heterochromatin is reinforced by the SET domain. *J Cell Biol* **170**, 537 (2005).

- 32 Stewart, M., Li, J. & Wong, J. Relationship between histone H3 lysine 9 methylation, transcription repression, and heterochromatin protein 1 recruitment. *Mol Cell Biol* **25**, 2525 (2005).
- 33 Hathaway, N. A., Bell, O., Hodges, C., Miller, E. L., Neel, D. S. & Crabtree, G. R. Dynamics and memory of heterochromatin in living cells. *Cell* **149**, 1447 (2012).
- 34 Brown, Z. Z., Müller, M. M., Kong, H. E., Lewis, P. W. & Muir, T. W. Targeted histone peptides: Insights into the spatial regulation of the methyltransferase PRC2 by using a surrogate of heterotypic chromatin. *Angew Chem Int Ed* **in press** (2015).
- 35 Johnson, A., Li, G., Sikorski, T. W., Buratowski, S., Woodcock, C. L. & Moazed, D. Reconstitution of Heterochromatin-Dependent Transcriptional Gene Silencing. *Mol Cell* **35**, 769 (2009).
- 36 Hall, I. M., Shankaranarayana, G. D., Noma, K.-I., Ayoub, N., Cohen, A. & Grewal, S. I. Establishment and maintenance of a heterochromatin domain. *Science* **297**, 2232 (2002).
- 37 Wu, H. *et al.* Structural biology of human H3K9 methyltransferases. *PloS one* **5** (2010).
- 38 Wang, T. *et al.* Crystal Structure of the Human SUV39H1 Chromodomain and Its Recognition of Histone H3K9me_{2/3}. *PloS one* **7** (2012).
- 39 Min, J., Zhang, X., Cheng, X., Grewal, S. I. & Xu, R.-M. M. Structure of the SET domain histone lysine methyltransferase Clr4. *Nat Struct Biol* **9**, 828 (2002).
- 40 Liu, N. *et al.* Recognition of H3K9 methylation by GLP is required for efficient establishment of H3K9 methylation, rapid target gene repression, and mouse viability. *Genes Dev* **29**, 379 (2015).
- 41 Li, S. & Shogren-Knaak, M. A. The Gcn5 bromodomain of the SAGA complex facilitates cooperative and cross-tail acetylation of nucleosomes. *J Biol Chem* **284**, 9411 (2009).
- 42 Nguyen, U. T. T., Bittova, L., Müller, M. M., Fierz, B., David, Y., Houck-Loomis, B., Feng, V., Dann, G. P. & Muir, T. W. Accelerated chromatin biochemistry using DNA-barcoded nucleosome libraries. *Nat Meth* **11**, 834 (2014).

- 43 Blanco-Canosa, J. B. & Dawson, P. E. An Efficient Fmoc-SPPS Approach for the Generation of Thioester Peptide Precursors for Use in Native Chemical Ligation. *Angew Chem Int Ed* **47**, 6851 (2008).
- 44 Wan, Q. & Danishefsky, S. J. Free-radical-based, specific desulfurization of cysteine: a powerful advance in the synthesis of polypeptides and glycopolypeptides. *Angew Chem Int Ed* **46**, 9248 (2007).
- 45 Dyer, P. N., Edayathumangalam, R. S., White, C. L., Bao, Y., Chakravarthy, S., Muthurajan, U. M. & Luger, K. Reconstitution of nucleosome core particles from recombinant histones and DNA. *Methods Enzymol* **375**, 23 (2004).
- 46 Dorigo, B., Schalch, T., Bystricky, K. & Richmond, T. J. Chromatin fiber folding: Requirement for the histone H4 N-terminal tail. *J Mol Biol* **327**, 85 (2003).
- 47 Fierz, B., Chatterjee, C., McGinty, R. K., Bar-Dagan, M., Raleigh, D. P. & Muir, T. W. Histone H2B ubiquitylation disrupts local and higher-order chromatin compaction. *Nat Chem Biol* **7**, 113 (2011).
- 48 Cheng, X. & Blumenthal, R. M. Coordinated chromatin control: Structural and functional linkage of DNA and histone methylation. *Biochemistry* **49**, 2999 (2010).
- 49 Sprague, B. L., Pego, R. L., Stavreva, D. A. & McNally, J. G. Analysis of binding reactions by fluorescence recovery after photobleaching. *Biophys J* **86**, 3473 (2004).

ACKNOWLEDGMENTS

We thank Dr. Uyen Nguyen and Dr. Yael David for help with tissue culture, Dr. Gary Laevsky for advice on microscopy, Dr. Peter Lewis for generously providing biotinylated H3 peptides, and Dr. David Allis, Dr. Galia Debelouchina, Dr. Zachary Brown, Boyuan Wang and Christopher Jenness for helpful discussions. Funding from the Swiss National Science Foundation (postdoctoral fellowships to M.M.M. and B.F.) and NIH (R01-GM107047) is gratefully acknowledged.

FIGURES

Figure 1

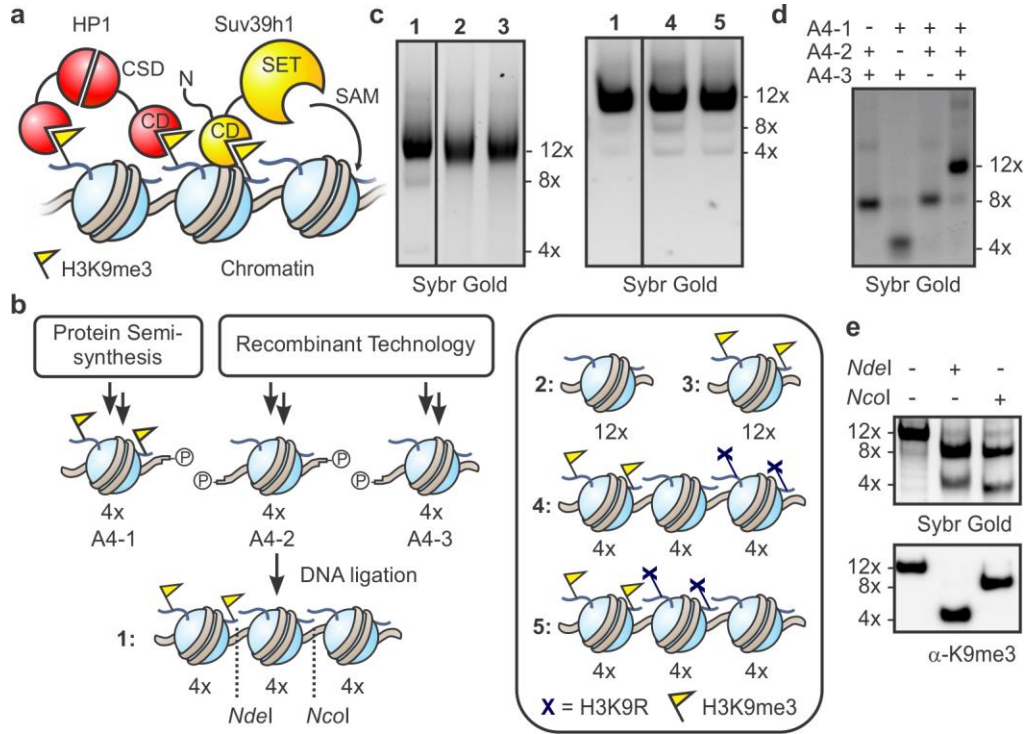


Figure 1: Heterotypic designer chromatin substrates. (a) Simplified model for heterochromatin spreading. H3K9me3-modified (yellow flags) nucleosomes serve to recruit the scaffolding protein HP1 and the histone methyltransferase (HMT) Suv39h1 through their chromodomains (CDs). The latter catalyzes the S-adenosylmethionine (SAM)-dependent methylation of H3K9 via its SET domain, thus providing a positive feedback loop. HP1 forms a dimer through interactions of its chromo-shadow domain (CSD). (b) Schematic for the synthesis of heterotypic designer nucleosome arrays. *NdeI* and *NcoI* sites for restriction analysis are indicated by dotted lines. See supporting information for more detail. Inset: cartoon representation of control arrays. (c) Purity of designer chromatin assessed by native gel electrophoresis. For additional data, see **Supplementary Fig. 1** in the supporting information. (d) Ligations of purified 4-mer arrays proceed selectively as indicated by native gel electrophoresis of crude products from ligation reactions of designated array fragments. (e) PTM-containing 'priming' domain remains intact through designer chromatin synthesis. Ligated arrays (**1**) were digested and the resulting fragments analyzed by native gel electrophoresis and western blotting for H3K9me3.

Figure 2

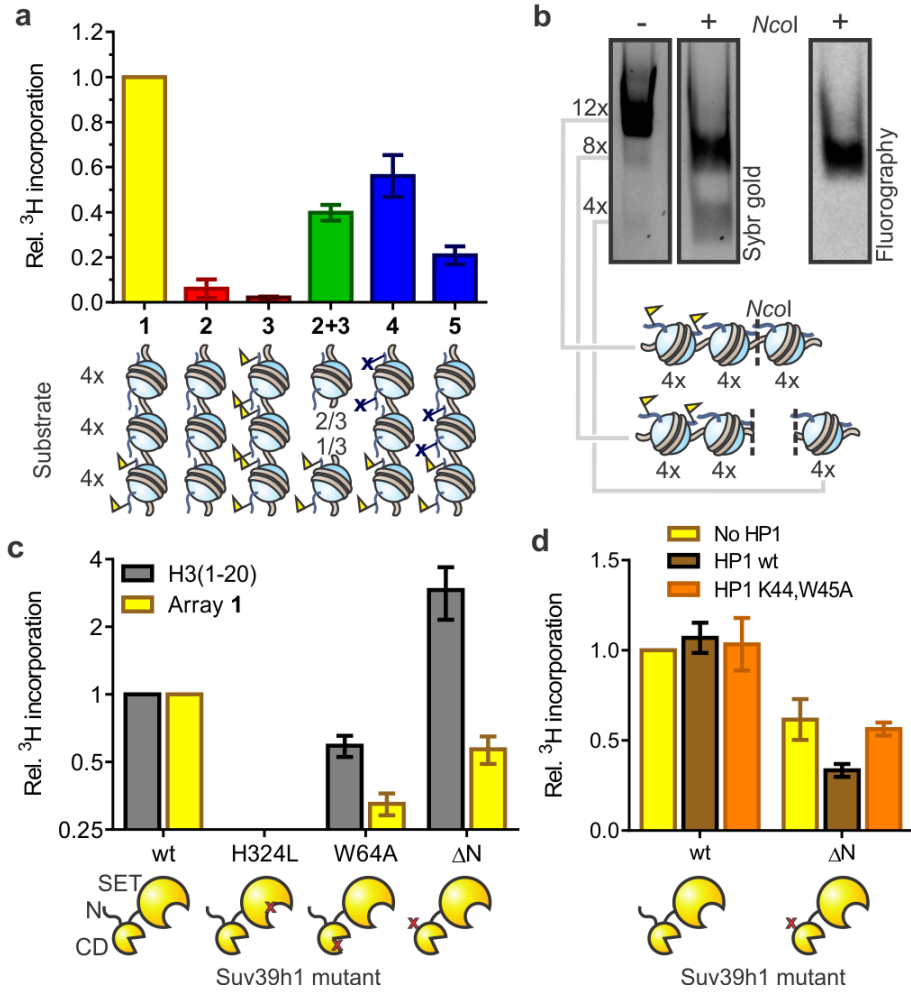


Figure 2: Reconstitution of Suv39h1-dependent heterochromatin spreading in vitro.

(a) Substrate preference of Suv39h1-catalyzed spreading. Arrays **2** and **3** represent homotypic templates (red) carrying either H3K9me0 or H3K9me3, respectively. Inter-fiber spreading is evaluated with a 2:1 mixture of arrays **2** and **3** (green) to match the stoichiometry of histones in array **1** (yellow). Arrays **4** and **5** (blue) contain H3K9R mutations to block spreading. HMT activity was measured using ^3H -SAM as the co-factor in the presence of 5 mM MgCl_2 . Scintillation counts are normalized to the values determined with heterotypic array **1**, without additional normalization for number of substrate sites. Error bars, s.e.m. (n = 3). (b) Suv39h1 preferentially methylates nucleosomes adjacent to preinstalled H3K9me3 marks. Arrays were methylated with ^3H -SAM in the presence of 0.5 mM MgCl_2 and subsequently digested with *NcoI*, separated by native gel electrophoresis and analyzed by Sybr gold staining (left) and fluorography (right). See **Supplementary Fig. 8** for more details. (c) HMT activity of Suv39h1 variants with an H3 peptide encompassing residues 1-20 (gray) or array **1** (yellow). Measurements are normalized to the values obtained with wild-type Suv39h1 and the respective substrate, and plotted on a log₂ scale. Error bars, s.e.m. (n = 3). (d) Impact of HP1 on methylation of array **1** by Suv39h1. Scintillation counts for assays in the presence of wild-type HP1 (brown) or the K44,W45A double mutant (orange, **Supplementary Fig. 2**) and indicated Suv39h1 variant are normalized to the values obtained for wt Suv39h1 in the absence of HP1 (yellow). Error bars, s.e.m. (n = 3-8).

Figure 3

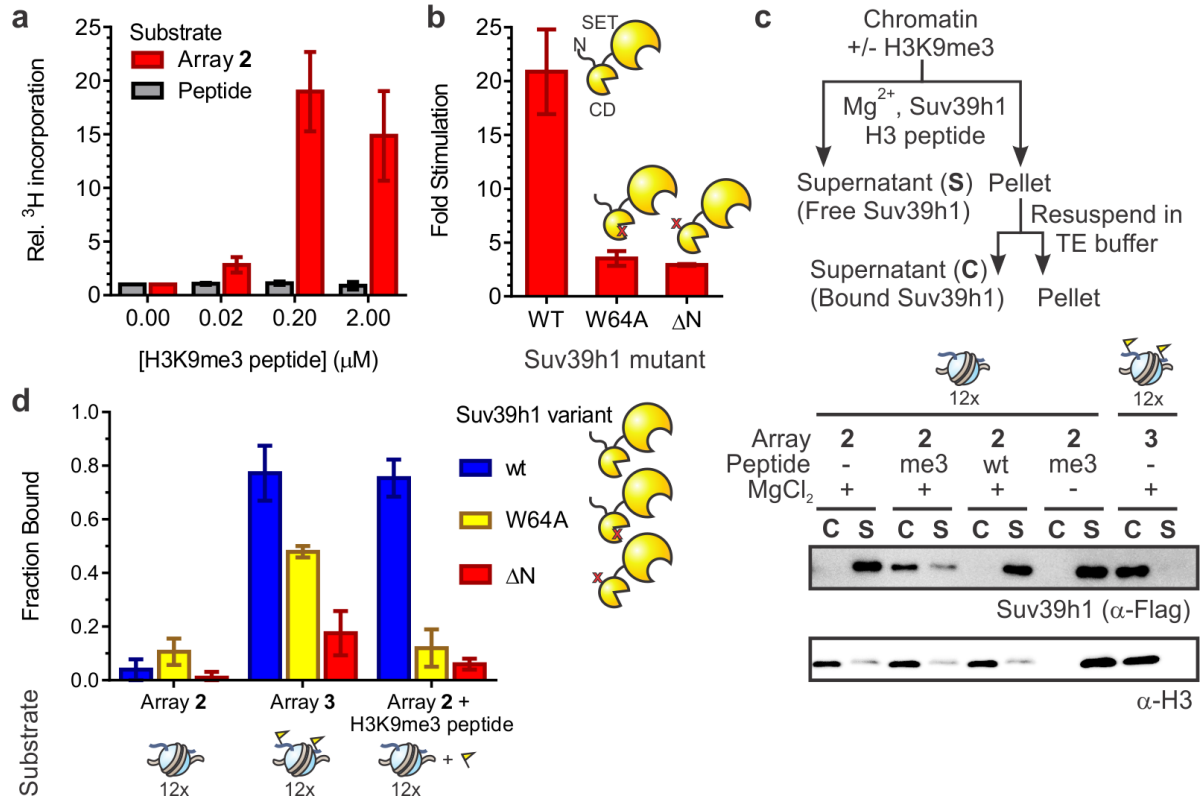


Figure 3: Trans-activation of Suv39h1. (a) Allosteric activation of Suv39h1 by H3K9me3 peptides occurs only on chromatin substrates. ³H-SAM-based HMT assays were performed on either unmodified peptide (gray) or array 2 (red) substrates in the presence of increasing amounts of H3K9me3 peptide added in *trans*. In each case, ³H-me incorporation was normalized to the value obtained in the absence of H3K9me3 peptide. Error bars, s.e.m. (n = 4). (b) Suv39h1-activation requires an intact chromodomain and N-terminus. Stimulation of HMT activity is defined as the ratio of scintillation counts obtained on unmodified chromatin 2 in the presence of 0.2 μM H3K9me3 peptide vs. its absence. Error bars, s.e.m. (n = 3). (c) The H3K9me3 mark promotes chromatin binding in *cis* and in *trans*. Western blot (α-Flag upper panel; α-H3, lower panel) of a binding assay of wild-type Suv39h1 with array 2 or 3. Where appropriate, H3 peptides are added at a concentration of 0.2 μM. A control reaction in the absence of MgCl₂ is included (lanes 7 and 8). (d) Chromatin binding is promoted by the H3K9me3 mark and requires an intact chromodomain and N-terminus. Bound fractions are determined by densitometry of Suv39h1 western blots (α-Flag) bands corresponding to the re-dissolved pellet (chromatin associated) and supernatant (unbound) of binding reactions. Error bars, s.e.m. (n = 3).

Figure 4

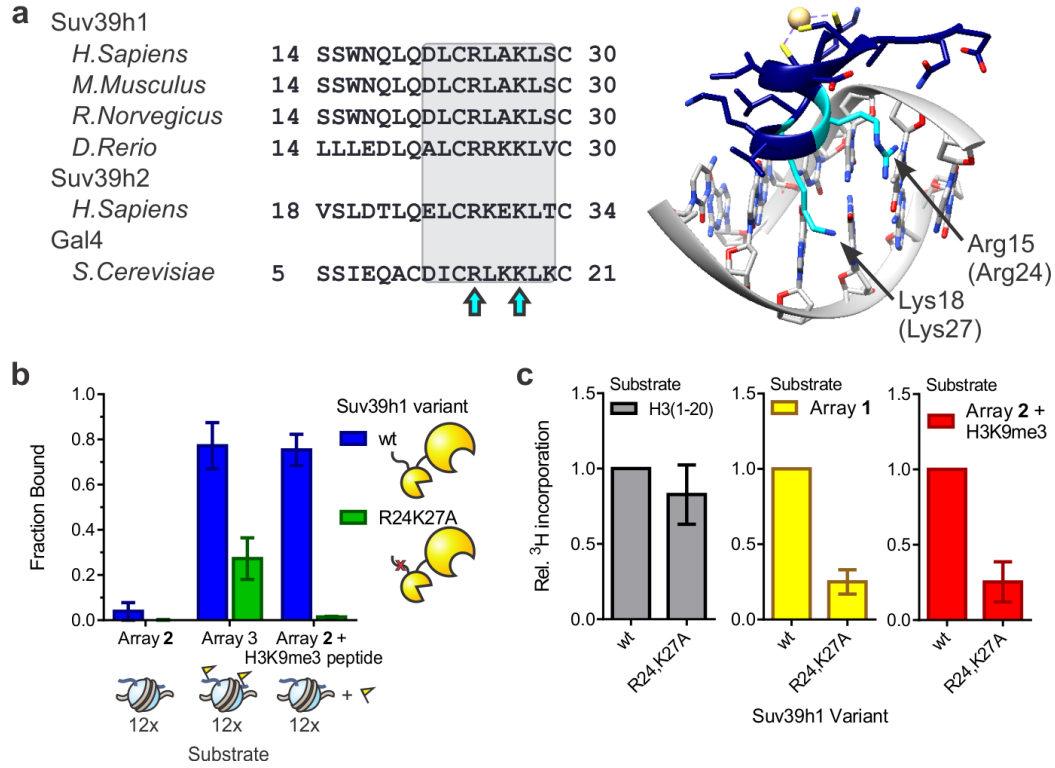


Figure 4: A Zinc-finger-like motif at the N-terminus of Suv39h1 contributes to chromatin binding. (a) Sequence alignment of the Suv39h1 N-terminus from indicated species reveals similarity with the DNA-binding helix of Gal4 (gray box). Cyan arrows denote Arg24 and Lys27, the putative DNA binding residues of Suv39h1. The structure of the Gal4 zinc-finger bound to DNA is shown on the right (pdb code: 1D66) with the DNA binding residues highlighted. (b) Residues R24 and K27 contribute to chromatin binding. Bound fractions are determined by densitometry of Suv39h1 western blots (α -Flag) bands corresponding to the re-dissolved pellet (chromatin associated) and supernatant (unbound) of co-precipitation reactions. Error bars, s.e.m. (n = 3). (c) The R24,K27A mutant displays reduced activity on chromatin substrates. HMT measurements with H3 peptides (left), array **1** (middle), or array **2** in the presence of 0.2 μ M H3K9me3 peptide (right) were normalized to the values obtained for wt Suv39h1. Error bars, s.e.m. (n = 5).

Figure 5

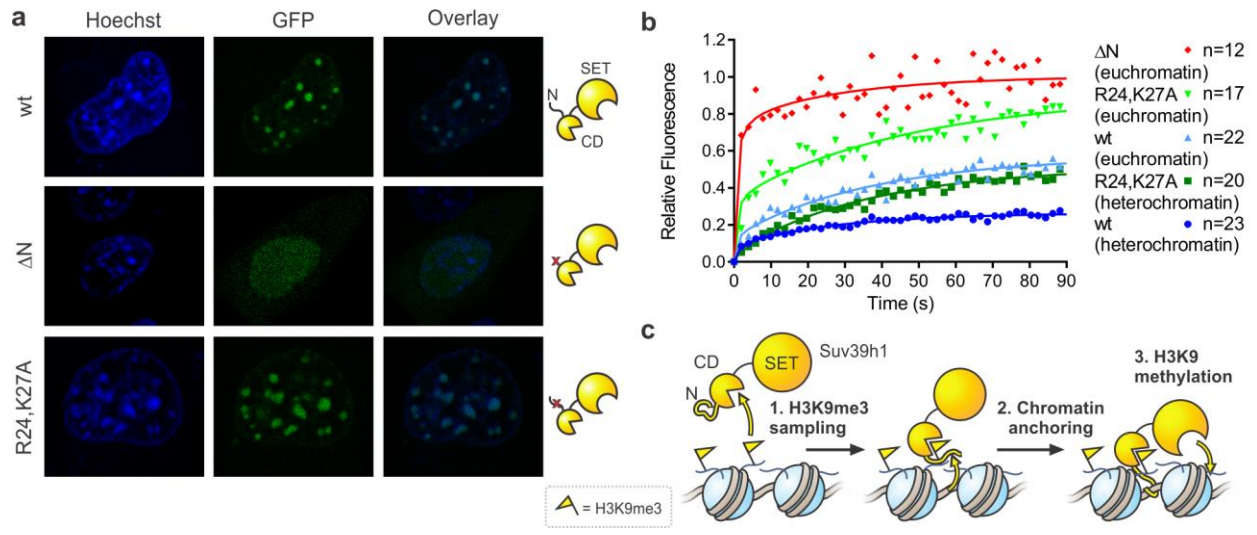


Figure 5: The Suv39h1 N-terminus contributes to chromatin binding *in vivo*. (a) Fluorescence microscopy images of indicated Suv39h1-GFP fusion proteins in NIH-3T3 cells. Cells were stained with Hoechst 33342 dye to visualize nuclei and heterochromatin foci. (b) FRAP analysis of Suv39h1-GFP fusion proteins in NIH-3T3 cells. FRAP profiles were recorded upon bleaching heterochromatin foci or a circular spot in the low intensity region of nuclei (euchromatin). For visualization purposes, the average of 12-23 individual measurements were fit to the coupled reaction-diffusion model of Sprague *et al.* ⁴⁹. (c) Model for a two-state activation of Suv39h1 methyltransferase activity. Freely diffusing Suv39h1 exhibits low HMT activity (left). Chromodomain (CD)-dependent recognition of nucleosomal H3K9me3 and subsequent anchoring to chromatin via the N-terminus of Suv39h1 (center; binding may occur to either linker or nucleosomal DNA) enhances HMT activity in the vicinity of the stimulating mark (right).

SUPPLEMENTARY MATERIALS

Supplementary methods

Figures S1-S13